Protein NMR Spectroscopy

DOI: 10.1002/ange.201310963

# Structural Mapping of a Chaperone–Substrate Interaction Surface**

*Morgane Callon, Björn M. Burmann, and Sebastian Hiller**

***Abstract:*** *NMR spectroscopy is used to detect site-specific intermolecular short-range contacts in a membrane–protein–chaperone complex. This is achieved by an "orthogonal" isotope-labeling scheme that permits the unambiguous detection of intermolecular NOEs between the well-folded chaperone and the unfolded substrate ensemble. The residues involved in these contacts are part of the chaperone–substrate contact interface. The approach is demonstrated for the 70 kDa bacterial Skp-tOmpA complex.*

Molecular chaperones play an essential role in the biogenesis of proteins in all kingdoms of life.[1,2] As a general mode of function, they interact with unfolded protein substrates, prohibiting their progression on non-native aggregation pathways.[3] Still, the molecular basis of chaperone–substrate interactions is not well understood at the atomic level.

NMR spectroscopy is a powerful technique to provide structural information of transient and dynamic protein–protein interactions at atomic resolution.[4,5] It has been successfully employed for the direct observation of substrates bound to the chaperones GroEL,[6–10] Hsp90,[11–13] Hsp70,[14] and Skp.[15,16] Furthermore, long-range spatial correlations between substrates and chaperones have been detected for Skp,[16] Hsp90,[11] and GroEL[10] by the use of paramagnetic relaxation enhancement (PRE). However, for a full description of the molecular interactions, the identification of direct contact interfaces in the unperturbed chaperone–substrate complex is necessary. Thereby, chemical shift perturbations do not necessarily yield the true interaction surface, because they are ensemble averages of the dynamic systems and can contain significant contributions of allosteric effects. Additional experimental approaches are thus required.

Herein, we use the nuclear Overhauser effect (NOE) to detect site-specific intermolecular short-range contacts in a membrane-protein–chaperone complex. We measure these contacts in the 70 kDa complex of the chaperone Skp with its bound substrate tOmpA. Skp is a homotrimeric, 51 kDa chaperone from the Gram-negative bacterium *Escherichia coli (E. coli)* that prevents outer membrane proteins from aggregation during their transport across the periplasm.[17,18] Its apo-form features three long α-helical "arms" forming a central cavity.[19] The 19 kDa transmembrane domain of the outer membrane protein A, tOmpA, is a natural substrate of Skp.[20] Previous solution NMR studies have shown that tOmpA and the alternative substrate OmpX, when bound to Skp, adopt the conformational state of a "fluid globule", a compacted ensemble of rapidly interconverting conformations devoid of regular secondary structure elements, but with non-random backbone dynamics.[16]

The interpretation of intermolecular cross-relaxation events between the folded Skp and the unfolded tOmpA has to consider that the $^1$H–$^1$H cross-relaxation rate constant $\sigma^{jk}$ between a proton $j$ on the chaperone and a proton $k$ on the substrate is an ensemble average (Supporting Information, Figure 1), similar to intramolecular NOEs in unfolded protein ensembles.[21–24] The amplitude of an NOE cross-peak between spin $j$ and $k$ thus contains contributions from different conformations of the structural ensemble, and importantly, owing to the $r^{-6}$ dependence of $\sigma^{jk}$, it is biased by conformations with short interspin distances $r$. Furthermore, as the dynamic ensemble features a narrow chemical shift dispersion, the observed cross-peaks in 3D NOESY spectra are typically a superimposition of multiple substrate spins with similar chemical shifts. These features generally prohibit a quantitative conversion of NOESY cross-peak amplitudes into interspin distances.

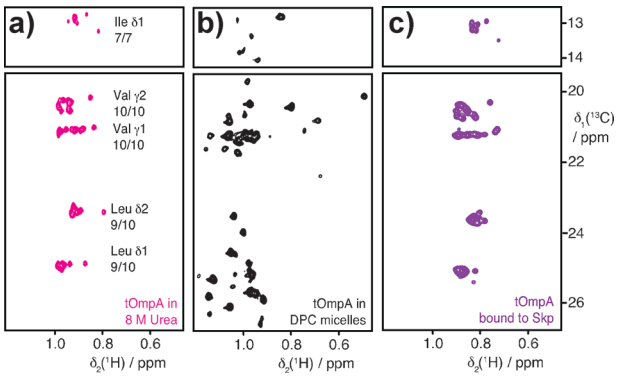


***Figure 1.*** Random-coil-like averaging of tOmpA side chain conformations in the Skp-bound state. a) 2D [$^{13}$C,$^1$H]-HSQC spectrum of 200 μM [*U*-$^2$H,$^{15}$N, Ile-δ1-$^{13}$CH$_3$, Leu,Val-$^{13}$CH$_3$]-tOmpA in NMR buffer with 8 M urea at 37 °C. The number of detected and expected resonances for each methyl moiety type are indicated. b) 2D [$^{13}$C,$^1$H]-HMQC spectrum of 550 μM [*U*-$^2$H,$^{15}$N, Ile-δ1-$^{13}$CH$_3$, Leu,Val-$^{13}$CH$_3$]-tOmpA in NMR buffer with 150 mM DPC at 37 °C. c) 2D [$^{13}$C,$^1$H]-HMQC spectrum of 560 μM [*U*-$^2$H,$^{15}$N, Ile-δ1-$^{13}$CH$_3$, Leu,Val-$^{13}$CH$_3$]-tOmpA bound to [*U*-$^2$H]-Skp in NMR buffer at 37 °C.

However, measurements of the NOE can be used to identify those residues of the chaperone that feature a significantly populated amount of conformations in close spatial

[*] M. Callon, Dr. B. M. Burmann, Prof. Dr. S. Hiller
Biozentrum, University of Basel
Klingelbergstrasse 70, 4056 Basel (Switzerland)
E-mail: sebastian.hiller@unibas.ch

[**] This work was supported by grants from the Swiss National Science Foundation (Grant PP00P3_128419) and the European Research Council (FP7 contract MOMP 281764) to S.H., and by a personal fellowship from the Werner-Siemens Foundation to M.C.

Supporting information for this article is available on the WWW under http://dx.doi.org/10.1002/anie.201310963.

  

contact with spin probes in the substrate. These residues are part of the chaperone–substrate contact surface. For mapping of these residues, we use an "orthogonal" side-chain labeling scheme, that is, a combination of amino acid side-chain moieties with non-overlapping $^{1}$H chemical shift dispersion. These are the methyl groups of isoleucine, leucine, and valine for the unfolded substrate (ILV-tOmpA) and the methyl groups of alanine residues for the chaperone (A-Skp), which were introduced in $^{13}CH_3$-labeled form on a deuterated background using established techniques.[25,26] Formation of the complex was accomplished by rapid dilution of purified, denatured tOmpA into separately produced Skp solution and subsequent buffer exchange. The integrity of the complex, its homogeneous 3:1 Skp:tOmpA stoichiometry, and the folding competence of tOmpA from the complex was assessed as described previously.[16]

A set of 2D [$^{13}$C,$^{1}$H]-correlation spectra of ILV-labeled tOmpA in three different preparational states serves as an initial characterization of the substrate side chains (Figure 1). In 8 M urea aqueous solution, tOmpA adopts a fast exchanging random-coil ensemble and accordingly, the ILV side chain moieties feature narrow $^{1}$H and $^{13}$C chemical shift dispersions of 0.22 ppm and 0.2–0.6 ppm, respectively (Figure 1 a). In the folded state of tOmpA in DPC micelles, the protein populates an 8-stranded β-barrel structure as the single, stable conformation. Therein, the ILV side chains are involved in specific contacts, resulting in $^{1}$H and $^{13}$C chemical dispersions about four times larger than in denaturant (Figure 1 b). Bound to the chaperone Skp, the methyl moieties of ILV-tOmpA feature again narrow chemical shift dispersions, closely resembling the random-coil spectrum and thus indicating that the tOmpA side-chains in Skp lack a well-defined structure (Figure 1 c). The observation of a single set of resonances confirms the presence of a conformational ensemble in the fast exchange regime, that is, with individual lifetimes below 1 ms, validating the use of an ensemble model as the basis of the data interpretation.

The alanine $CH_3$ resonances in Skp feature a large dispersion, both in the apo and the holo form, in accordance with the adoption of a well-defined secondary and tertiary structure (Figure 2 a). Intermolecular cross-peak amplitudes were measured by 3D $^{13}$C-resolved [$^{1}$H,$^{1}$H]-NOESY experiments. Importantly, the orthogonal side-chain labeling pattern ensures the absence of spectral overlap between the intermolecular cross-peaks and the strong diagonal peaks, as well as between inter- and intramolecular cross-peaks (Figure 2 b). The observation of a cross-peak in the isoleucine, leucine, and valine $^{1}$H chemical shift range 0.55–0.9 ppm in the holo- relative to the apo-spectrum can thus be directly assigned to intermolecular NOE contacts between a specific site on Skp and the ILV methyl spins in the tOmpA ensemble (Figure 2 c,d). The integration of alanine NOE cross-peaks shows non-zero cross-peak amplitudes for residues A34, A75, A78, and A86, all of which have their side-chains pointing into the central part the Skp cavity (Supporting Information, Table S1). Alanine residues located at the trimer interface, as well as at the bottom of Skp, did not show a detectable NOE to the spin probes in the substrate ensemble. The contact surface mapping thus shows that tOmpA is bound in the

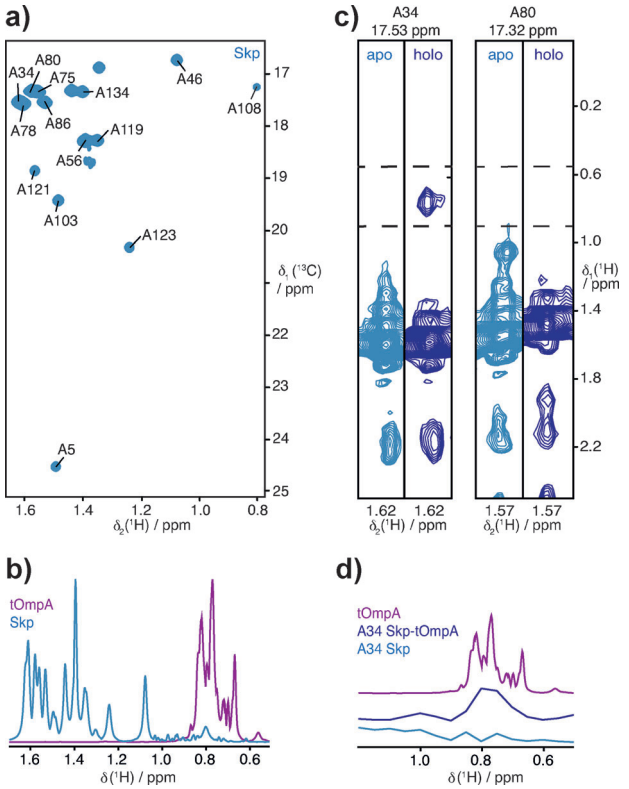


***Figure 2.*** Measurement of intermolecular methyl–methyl NOEs between Skp and tOmpA. a) 2D [$^{13}$C,$^{1}$H]-HMQC spectrum of 700 μM [*U*-$^{2}$H,$^{15}$N, Met-$^{13}CH_3$, Ala-$^{13}CH_3$]-Skp (A-Skp; light blue) in NMR buffer at 37 °C. The sequence-specific resonance assignments are indicated. b) Overlay of $^{1}$H projections of a 2D [$^{13}$C,$^{1}$H]-HMQC spectrum of 560 μM [*U*-$^{2}$H,$^{15}$N, Ile-δ1-$^{13}CH_3$, Leu,Val-$^{13}CH_3$]-tOmpA (ILV-tOmpA) bound to [*U*-$^{2}$H]-Skp in NMR buffer at 37 °C (purple) and of a 2D [$^{13}$C,$^{1}$H]-HMQC spectra of 700 μM A-Skp in NMR buffer at 37 °C (blue). c) 2D strips from 3D $^{13}$C-edited-[$^{13}$C,$^{1}$H]-NOESY spectra taken at the positions of Ala 34 and Ala 80 of 700 μM A-Skp in its apo form (light blue) and 250 μM A-Skp with bound ILV-tOmpA (holo form, dark blue) in NMR buffer at 37 °C. Spectra were recorded with a NOESY mixing time of 200 ms. The dashed horizontal lines indicate the $^{1}$H chemical shift dispersion of ILV residues in tOmpA bound to Skp (0.55–0.9 ppm). d) Overlay of a $^{1}$H projection of a 2D [$^{13}$C,$^{1}$H]-HMQC spectrum of 560 μM ILV-tOmpA bound to Skp (purple) and 1D cross sections from the 3D $^{13}$C-edited-[$^{13}$C,$^{1}$H]-NOESY spectra shown in (c), taken at the position of Ala 34.

central part of the Skp cavity (Figure 3). Notably, these intermolecular cross-peaks have the same sign as the diagonal peaks, indicating an overall negative NOE for the ensemble average and thus the existence of the slow motion limit for the chaperone–substrate contacts.[27,28] The local lifetimes of segments of the substrate bound to the chaperone thus have a lower limit of $\tau_i \gg \omega_0^{-1} \approx 1$ ns. A comparison to cross-peaks with known intramolecular distances within Skp in the same spectrum shows that the ensemble-averaged intensities correspond to fully populated distances in the range 5–6 Å (Supporting Information, Table S2). Since the intermolecular NOE peaks are a superposition of individual signals from up to 45 spin probes in tOmpA, we estimate that, on average, conformations with a given Skp–tOmpA $^{1}$H–$^{1}$H spin pair in close contact are populated by about 0.5–2 %.

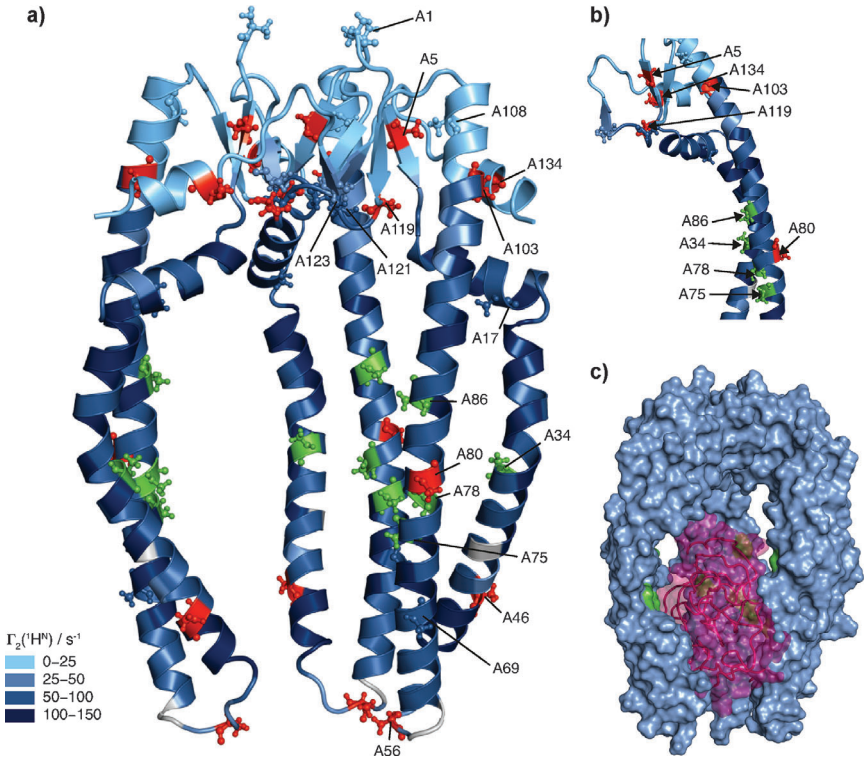


***Figure 3.*** The contact interface of tOmpA and Skp. a) Ribbon representation of the Skp crystal structure with the alanine residues shown as ball and sticks (PDB 1SG2).[19] Alanines shown in green and red correspond to residues with and without a significant intermolecular cross-peak in the 3D $^{13}$C-edited-[$^{13}$C,$^{1}$H]-NOESY spectrum of Skp bound to tOmpA, respectively (Supporting Information, Table S1). Intermolecular PREs on Skp from a paramagnetic spin label attached to OmpX are indicated by a blue gradient for $\Gamma_2$-values between 0 and 150 s$^{-1}$.[16] b) Zoom on one Skp monomer. c) Structural model of a single conformation from the dynamic Skp-tOmpA ensemble. Skp is shown in surface representation (blue). A randomly generated tOmpA polypeptide conformation is shown in purple.[16] Alanine residues with significant NOE cross-peak amplitude, as in (a), are highlighted in green.

Finally, we compare the result from the NOE-based mapping with previous measurements of intermolecular PREs from a paramagnetic spin label attached to OmpX and detected on the individual amide moieties of Skp.[16] Overall, the positions of the Omp substrate in the center of the Skp cavity determined by the two different spin-interaction methods PRE and NOE are in excellent agreement (Figure 3a). Importantly, however, the NOE mapping distinguishes residues A46 and A80, which are located in the Skp arms at the mid-height of the cavity, but with their side-chains pointing outside, from residues A34 and A78, which have both close contacts to tOmpA. The PRE, in turn, is similar for all four residues with $\Gamma_2$-values in the range 70–130 s$^{-1}$. The NOE-based contact interface mapping thus shows that the helical arms of Skp do not twist from their canonical position in the crystal structure and that they have a distinct substrate interaction surface on their inside.

In summary, measurements of intermolecular NOE in combination with a suitable orthogonal methyl group labeling strategy enabled the structural mapping of the Skp–tOmpA contact interface at the atomic level. Structurally meaningful intermolecular NOEs in the slow motion limit were detected in a folded–unfolded protein–protein complex. In particular, and compared to the long-ranged PREs, the short-ranged NOEs allow the distinction of residues according to their side-chain orientation. The approach can be tailored to a system of interest by suitable orthogonal combinations of methyl-group side chains. For example, methionine $CH_3$ moieties with proton signals from 1.95 to 2.25 ppm could be readily integrated in the present setup. Since methyl groups on a deuterated background are highly sensitive and since sequence-specific resonance assignments are known for molecular sizes larger than 150 kDa,[29,30] we estimate that with 70 kDa, the size limitation of the approach has not been reached in the present study. The approach thus opens new perspectives for the investigation of molecular interactions in protein biogenesis.

## Experimental Section

Details on protein biochemistry, isotope labeling and NMR spectroscopy are given in the Supporting Information. Sequence-specific side-chain resonance assignments of apo- and holo-Skp have been deposited to the BMRB data base with accession codes 19733 and 19730, respectively.

Received: December 18, 2013
Revised: February 17, 2014
Published online: April 2, 2014

**Keywords:** chaperone proteins · membrane proteins · NMR spectroscopy · protein ensembles · protein–protein interactions

[1] R. J. Ellis, S. M. van der Vies, *Annu. Rev. Biochem.* **1991**, *60*, 321–347.
[2] Y. E. Kim, M. S. Hipp, A. Bracher, M. Hayer-Hartl, F. U. Hartl, *Annu. Rev. Biochem.* **2013**, *82*, 323–355.
[3] S. M. Doyle, O. Genest, S. Wickner, *Nat. Rev. Mol. Cell Biol.* **2013**, *14*, 617–629.
[4] A. M. Bonvin, R. Boelens, R. Kaptein, *Curr. Opin. Chem. Biol.* **2005**, *9*, 501–508.
[5] J. Y. Suh, M. Cai, D. C. Williams, Jr., G. M. Clore, *J. Biol. Chem.* **2006**, *281*, 8939–8949.
[6] R. Horst, E. B. Bertelsen, J. Fiaux, G. Wider, A. L. Horwich, K. Wüthrich, *Proc. Natl. Acad. Sci. USA* **2005**, *102*, 12748–12753.
[7] E. Koculi, R. Horst, A. L. Horwich, K. Wüthrich, *Protein Sci.* **2011**, *20*, 1380–1386.
[8] Z. Wang, H. Feng, S. J. Landry, J. Maxwell, L. M. Gierasch, *Biochemistry* **1999**, *38*, 12537–12546.

  

[9] M. Yagi-Utsumi, T. Kunihara, T. Nakamura, Y. Uekusa, K. Makabe, K. Kuwajima, K. Kato, *FEBS Lett.* **2013**, *587*, 1605 – 1609.
[10] D. S. Libich, N. L. Fawzi, J. Ying, G. M. Clore, *Proc. Natl. Acad. Sci. USA* **2013**, *110*, 11361 – 11366.
[11] F. Hagn, S. Lagleder, M. Retzlaff, J. Rohrberg, O. Demmer, K. Richter, J. Buchner, H. Kessler, *Nat. Struct. Mol. Biol.* **2011**, *18*, 1086 – 1093.
[12] S. J. Park, B. N. Borin, M. A. Martinez-Yamout, H. J. Dyson, *Nat. Struct. Mol. Biol.* **2011**, *18*, 537 – 542.
[13] S. Rüdiger, S. M. V. Freund, D. B. Veprintsev, A. R. Fersht, *Proc. Natl. Acad. Sci. USA* **2002**, *99*, 11085 – 11090.
[14] S. Y. Stevens, S. Cai, M. Pellecchia, E. R. Zuiderweg, *Protein Sci.* **2003**, *12*, 2588 – 2596.
[15] T. A. Walton, C. M. Sandoval, C. A. Fowler, A. Pardi, M. C. Sousa, *Proc. Natl. Acad. Sci. USA* **2009**, *106*, 1772 – 1777.
[16] B. M. Burmann, C. Wang, S. Hiller, *Nat. Struct. Mol. Biol.* **2013**, *20*, 1265 – 1272.
[17] N. Ruiz, D. Kahne, T. J. Silhavy, *Nat. Rev. Microbiol.* **2006**, *4*, 57 – 66.
[18] J. G. Sklar, T. Wu, D. Kahne, T. J. Silhavy, *Genes Dev.* **2007**, *21*, 2473 – 2484.
[19] I. P. Korndörfer, M. K. Dommel, A. Skerra, *Nat. Struct. Mol. Biol.* **2004**, *11*, 1015 – 1020.
[20] S. Jarchow, C. Lück, A. Görg, A. Skerra, *Proteomics* **2008**, *8*, 4987 – 4994.
[21] K. Wüthrich, *Curr. Opin. Struct. Biol.* **1994**, *4*, 93 – 99.
[22] K. M. Fiebig, H. Schwalbe, M. Buck, L. J. Smith, C. M. Dobson, *J. Phys. Chem.* **1996**, *100*, 2661 – 2666.
[23] E. Barbar, *Biopolymers* **1999**, *51*, 191 – 207.
[24] K. A. Crowhurst, J. D. Forman-Kay, *Biochemistry* **2003**, *42*, 8687 – 8695.
[25] N. K. Goto, K. H. Gardner, G. A. Mueller, R. C. Willis, L. E. Kay, *J. Biomol. NMR* **1999**, *13*, 369 – 374.
[26] S. R. Tzeng, M. T. Pai, C. G. Kalodimos, *Methods Mol. Biol.* **2012**, *831*, 133 – 140.
[27] R. R. Ernst, G. Bodenhausen, A. Wokaun, *Principles of Nuclear Magnetic Resonance in One and Two Dimensions*, Clarendon, Oxford, **1987**.
[28] K. Wüthrich, *NMR of Proteins and Nucleic Acids*, Wiley, New York, **1986**.
[29] I. Gelis, A. M. Bonvin, D. Keramisanou, M. Koukaki, G. Gouridis, S. Karamanou, A. Economou, C. G. Kalodimos, *Cell* **2007**, *131*, 756 – 769.
[30] R. Rosenzweig, S. Moradi, A. Zarrine-Afsar, J. R. Glover, L. E. Kay, *Science* **2013**, *339*, 1080 – 1083.

  